before falling rapidly as one approaches the hcp or bcc phase of the pure metals Ti or Zr. The experimental values of $D(\epsilon_F)$ for the alloys can be compared with those of a calculation of $D(\epsilon)$ for bcc Nb by assuming the rigid band model (see fig. 9). Alloying with Zr lowers ϵ_F of Nb so that ϵ_F lies closer to a peak in the $D(\epsilon)$ function for bcc transition metals. Thus $D(\epsilon_F)$ is increased by alloying; in addition, also note that θ_D is decreased on alloying by comparison with θ_D for either pure Zr or pure Nb. This suggests that $\langle\omega^2\rangle$ is decreased on alloying. Both the change in $D(\epsilon_F)$ and $\langle\omega^2\rangle$ should have the result of increasing λ [see eq. (6)]. Thus we can understand the enhancement of T_c by alloying. In §4.2 it will be noted that Nb–Zr alloys are prone to an allotropic phase transformation at elevated temperatures. The allotropic phase is referred to as the ω-phase. The general softening of phonons evidenced by the minimum in θ_D for these alloys may be in part due to the softening of a particular set of phonon modes involved in the ω-phase transformation (see ch. 15).

A second example of an alloying effect is also given in table 3. When one alloys Mo with Re to form a bcc solid solution, one observes a dramatic increase in T_c. Again, this can be correlated with a rise in $D(\epsilon_F)$ and a lowering of the Debye temperature as seen in the table. Again, these effects are characterized by a destabilization of the bcc lattice and accompanying softening of phonon frequencies. Figure 12 illustrates the composition dependence of T_c, $D(\epsilon_F)$, θ_D^2, and λ. This figure shows very clearly the reciprocal relationship between λ and $\langle\omega^2\rangle \sim (\theta_D^2)$ as well as the direct correlation of both T_c and λ with $D(\epsilon_F)$.

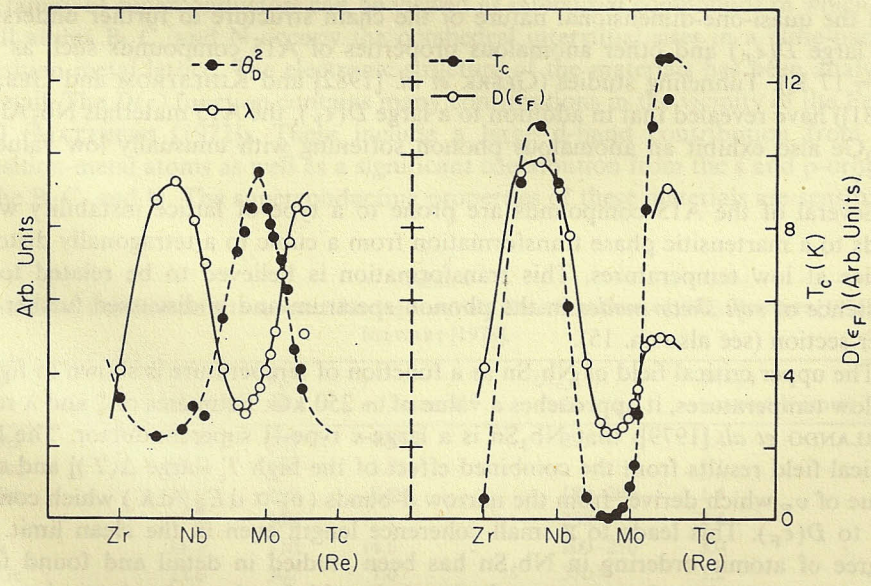

Fig. 12. The variation with group number of θ_D^2, λ (left-hand side) and T_c and $D(\epsilon_F)$ (right-hand side) for bcc transition metals and solid solutions of neighboring metals of the 4d-series. Data for Mo–Re solutions (group VI–group VII) are used in place of Mo–Tc alloys since data of Tc alloys is lacking.

References: p. 1776.

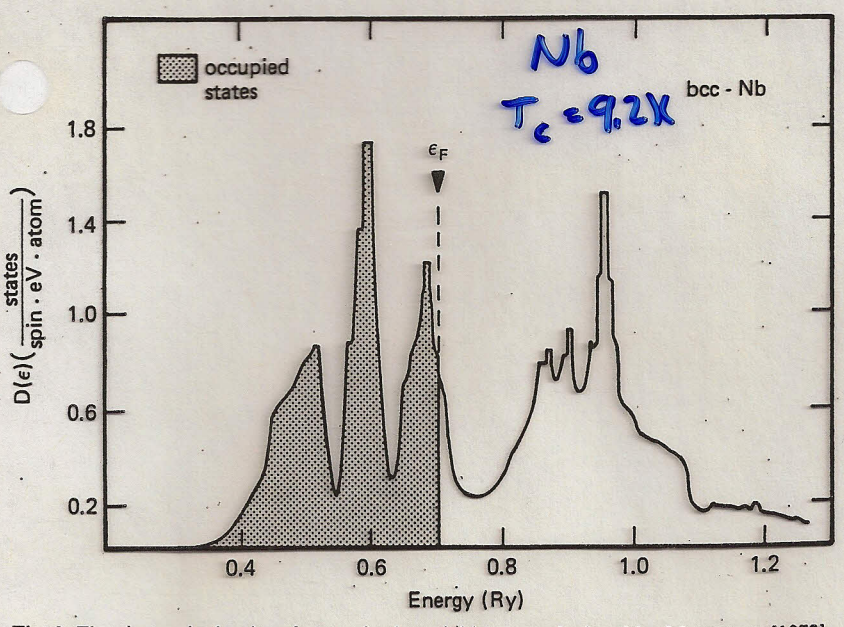

Fig. 9. The electronic density of states for bcc niobium as calculated by MATTHEISS [1972].

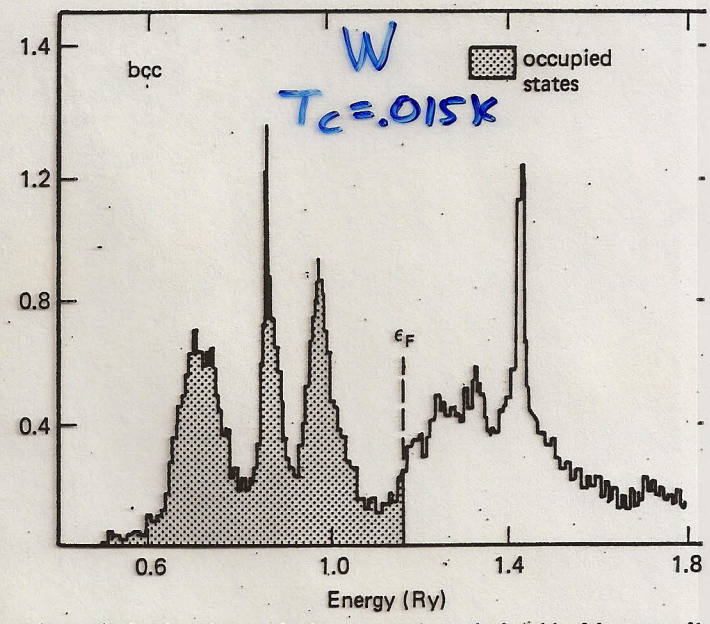

ıe electronic density of states for bcc tungsten as calculated by MATTHEISS [1

$\gamma \sim N(E_F)$

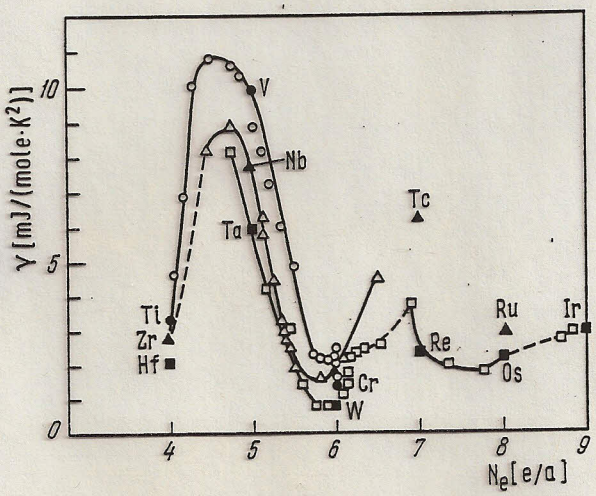

Fig.5.8. The dependence of γ on N_e in solid solutions formed by neighbouring transition 3d(o), 4d(Δ) and 5d (□) metals. The dark symbols correspond to pure metals

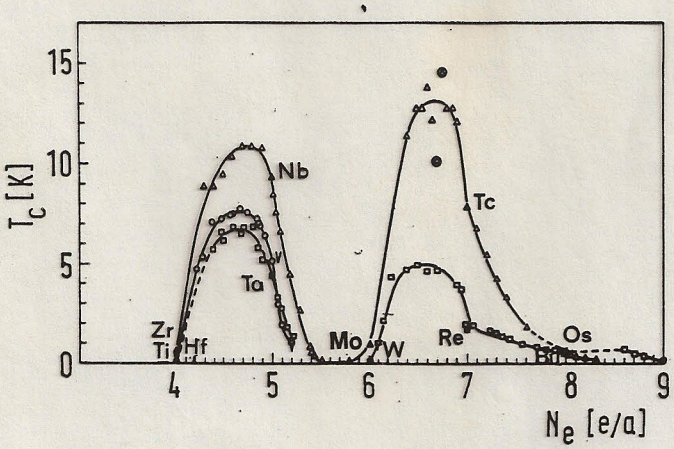

$T_c \sim \omega_D e^{-1/NV}$

Fig.5.10. The dependence of T_c on the number of valence electrons, N_e, in solid solutions formed by neighbouring transition metals. The legend is the same as in Fig.5.8